BCL-2 and Mutant NRAS Interact Physically and Functionally in a Mouse Model of Progressive Myelodysplasia

Nader Omidvar,[1,4] Scott Kogan,[6] Stephanie Beurlet,[1] Carole le Pogam,[1] Anne Janin,[1] Robert West,[5] Maria-Elena Noguera,[1] Murielle Reboul,[1] Annie Soulie,[1] Christophe Leboeuf,[1] Niclas Setterblad,[1] Dean Felsher,[7] Eric Lagasse,[8] Azim Mohamedali,[9] N. Shaun B. Thomas,[9] Pierre Fenaux,[2] Michaela Fontenay,[3] Marika Pla,[1] Ghulam J. Mufti,[9] Irving Weissman,[7] Christine Chomienne,[1] and Rose Ann Padua[1]

[1]Institut National de la Sante et de la Recherche Medicale U718 and 728, Université Paris 7 Denis Diderot, Faculté de Médicine, Institut Universitaire d'Hématologie-IFR105, AP-HP, Hôpital Saint-Louis; [2]Service d'Hématologie Clinique, Hôpital Avicenne (AP-HP)/Université Paris 13; [3]Département d'Hématologie, Institut Cochin, Hôpital Cochin, Paris, France; Schools of [4]Biosciences and [5]Medicine, Cardiff University, Cardiff, United Kingdom; [6]University of California, San Francisco, California; [7]Stanford University, Stanford, California; [8]McGowan Institute of Regenerative Medicine, Pittsburgh, Pennsylvania; and [9]Department of Haematological Medicine, Guy's, King's and Saint Thomas' School of Medicine, London, United Kingdom

Abstract

Myelodysplastic syndromes (MDS) are clonal stem cell hematologic disorders that evolve to acute myeloid leukemia (AML) and thus model multistep leukemogenesis. Activating *RAS* mutations and overexpression of *BCL-2* are prognostic features of MDS/AML transformation. Using *NRASD12* and *BCL-2*, we created two distinct models of MDS and AML, where human (h)BCL-2 is conditionally or constitutively expressed. Our novel transplantable *in vivo* models show that expression of hBCL-2 in a primitive compartment by mouse mammary tumor virus–long terminal repeat results in a disease resembling human MDS, whereas the myeloid MRP8 promoter induces a disease with characteristics of human AML. Expanded leukemic stem cell ($Lin^-/Sca\text{-}1^+/c\text{-}Kit^+$) populations and hBCL-2 in the increased RAS-GTP complex within the expanded $Sca\text{-}1^+$ compartment are described in both MDS/AML–like diseases. Furthermore, the oncogenic compartmentalizations provide the proapoptotic versus antiapoptotic mechanisms, by activating extracellular signal-regulated kinase and AKT signaling, in determination of the neoplastic phenotype. When hBCL-2 is switched off with doxycycline in the MDS mice, partial reversal of the phenotype was observed with persistence of bone marrow blasts and tissue infiltration as RAS recruits endogenous mouse (m)BCL-2 to remain active, thus demonstrating the role of the complex in the disease. This represents the first *in vivo* progression model of MDS/AML dependent on the formation of a BCL-2:RAS-GTP complex. The colocalization of BCL-2 and RAS in the bone marrow of MDS/AML patients offers targeting either oncogene as a therapeutic strategy. [Cancer Res 2007;67(24):11657–67]

Introduction

Leukemogenesis is a multistep process involving abnormalities in the expression or function of proteins encoded by a number of genes (reviewed in refs. 1–3). These abnormalities control the balance between cell proliferation, apoptosis, and differentiation, with dysregulation of these genes in hematopoietic malignancies leading to an expansion of abnormal stem cells. Abnormalities in certain stem cell genes are needed to dysregulate cell proliferation and also to bypass controls that would normally trigger apoptosis, differentiation, or senescence (4). Combinations of oncogenes that transform mouse cells and transgenic models of various malignancies have been described (5, 6). However, few studies have analyzed the progression of genetic events leading to the expansion of the leukemic clone. Approximately 30% of myelodysplastic syndrome (MDS) patients evolve to acute myelogenous leukemia (AML). This progressive and indolent evolution suggests the acquisition of several gene abnormalities.

Mutations of *NRAS* can occur in patients at risk of leukemia transformation after chemotherapy and/or radiotherapy (7, 8). We and others have shown that *NRAS* mutations at codon 12 is the most frequent molecular abnormality in MDS and is linked to poor survival and transformation to AML (9–11). The effect of mutant *RAS* is structure and cell context dependent. The family of RAS proteins includes HRAS, KRAS, and NRAS, whose oncogenic potential can be activated by point mutations in the GTP-binding domains around codons 12 and 61. The biological consequences of expressing mutant *NRASD12 in vitro* in human primary $CD34^+$ cells include impairment of proliferation, increased cell cycle time, and increased apoptosis (12). Likewise, in murine hematopoietic FDC-P1 cells, mutant *NRASD12* induces proliferation and reduced growth factor dependence *in vitro* (13). When MDS transforms into AML, the increased apoptosis seen in low-risk refractory anemia MDS patients' $CD34^+$ cells is reduced and an increase of antiapoptotic signals is observed. Cell biology and iron kinetic studies have shown that proliferation of the stem cell is linked with intramedullary cell death (14), which explains the ineffective hematopoiesis and often hypercellular marrow (15). As *BCL-2* has been observed to be up-regulated in AML patients (16, 17) and blocks differentiation of myeloid progenitors (18), it may be considered as a potential candidate progression gene of MDS transformation. Indeed, mouse models involving members of the BCL-2 family such as the proapoptotic BID-deficient mice develop an MDS-chronic myelomonocytic leukemia–like disease (19).

We hypothesized that the combined expression of *BCL-2* and mutant *NRAS* would establish a mouse model of progression to leukemia. Thus, herein, we describe two distinguishable high-penetrance *in vivo* models of MDS and AML. Furthermore, by

Note: Supplementary data for this article are available at Cancer Research Online (http://cancerres.aacrjournals.org/).

Requests for reprints: Rose Ann Padua, Institut Universitaire d'Hématologie-IFR105, Institut National de la Sante et de la Recherche Medicale UMR-S-718, Laboratoire d'Hématologie Paris, Paris, France. Phone: 33-1-53-72-40-72; Fax: 33-1-53-72-40-16; E-mail: padua@stlouis.inserm.fr.

doi:10.1158/0008-5472.CAN-07-0196

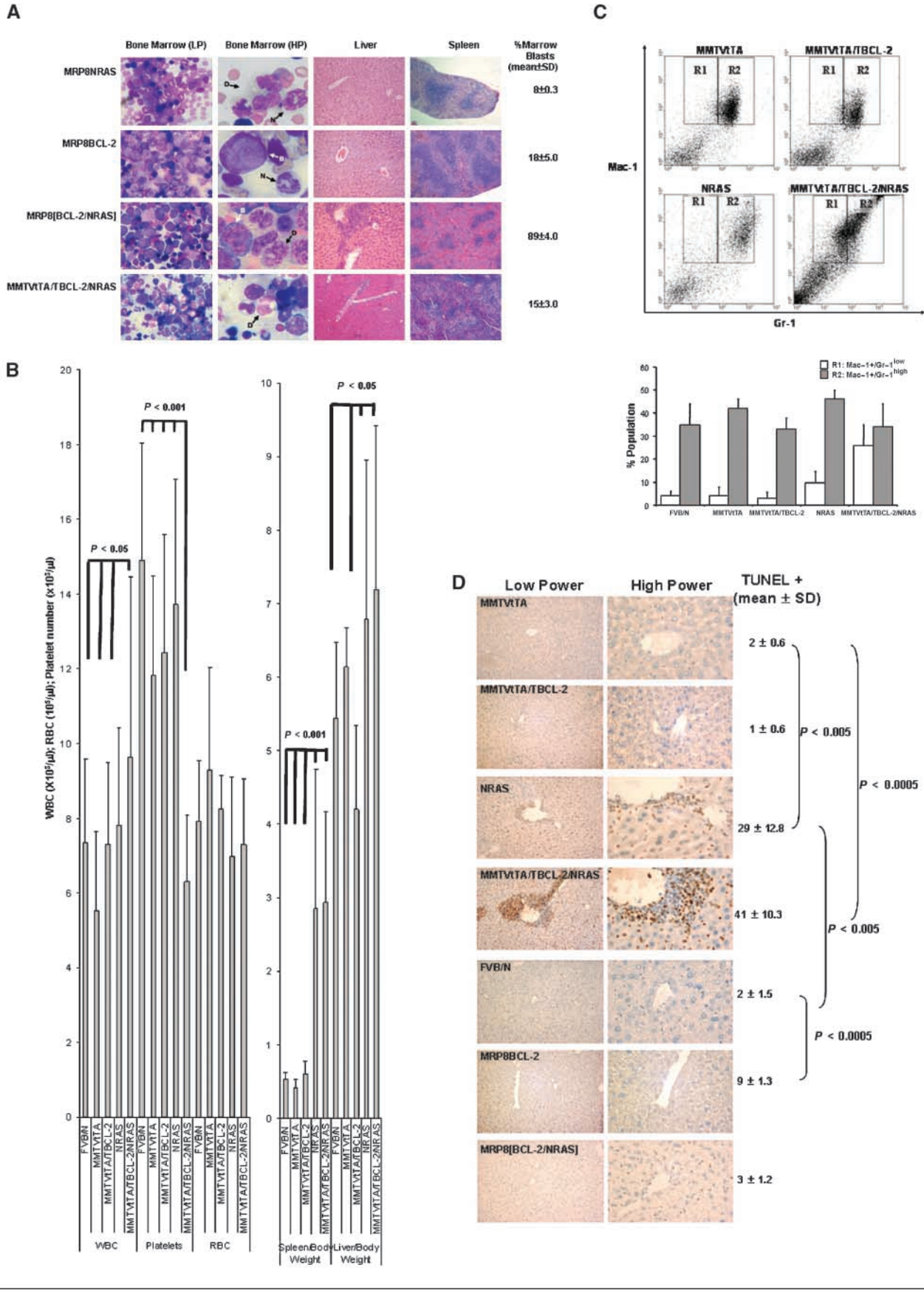

taking advantage of the conditional tetracycline-inducible system, we show that the triple transgenic *MMTVtTA/TBCL-2/NRASD12* develop an MDS with increased blasts and that BCL-2 expression is necessary for both initiating this neoplasm and for fatal disease progression. We provide mechanistic evidence of the colocalization and complexing of BCL-2 with active-RAS, which we also see in MDS/AML patients, and show different signaling pathways between the two models.

Materials and Methods

Transgenic mice. Generations of transgenic mice are described in detail in Supplementary Experimental Procedures. All procedures complied with European or national regulations.

Tissue and cell preparation. Blood was obtained from anesthetized animals (with isoflurane) by venipuncture of retro-orbital venus plexus into EDTA tubes. Differential blood counts were obtained using an automated hematology analyzer running veterinary software (Hemavet 850, CDC Technologies). Bone marrow was obtained by flushing long bones with HBSS followed by filtering through a nylon mesh. Blood and bone marrow smears were prepared according to standard hematologic techniques. Bone marrow smears were examined by cytologists from the Cardiff School of Medicine, King's College Hospital and Hôpital Saint-Louis. The tissue sections were examined by the Head of Histopathology of Hôpital Saint-Louis, and classified according to the Bethesda proposal (20) where blast equivalents are designated as "immature forms/blasts," which for the purposes of convenience are referred to as blasts herein. Percentage blasts were determined from the bone marrow smears by counting 100 to 200 cells. Lin^-, $Sca\text{-}1^+$ (marker of early progenitor), and $Mac\text{-}1^+$ (integrin equivalent of human CD11b) fractions were separated using an AutoMacs separator (Miltenyi). The lineage depletion kit contained a mixture of biotinylated antibodies CD5 (T-cell antigen), CD45R (lymphocyte antigen), Mac-1, Gr-1(Lys-6G) (granulo-macrophagic differentiation antigens), and Ter119 (early erythroid antigen). Cell sorting for $Lin^-/Sca\text{-}1^+/c\text{-}Kit^+$ bone marrow cells were undertaken using anti–Sca-1 antibody conjugated with FITC and anti–c-Kit antibody conjugated with allophycocyanin (Becton Dickinson). Cell sorting was undertaken using an LSR (Becton Dickinson). Livers and spleens were fixed overnight in buffered formalin and embedded in paraffin and sectioned by the Moffit Hospital, University of California San Francisco or Hôpital Saint-Louis, IUH Histopathology departments.

Immunophenotyping by flow cytometry. Mice were anesthetized with isoflurane and peripheral blood samples were obtained by orbital bleeds using EDTA as anticoagulant. Twenty-five microliter aliquots of peripheral blood cells were immunophenotyped with antibodies conjugated with either phycoerythrin or FITC. Bone marrow and spleen cells were analyzed using Sca-1, c-Kit, Mac-1, Gr-1, B220 (B cell), and CD3 (T cell; Becton Dickinson). When required, cells were permeabilized with "Fix and Perm" (Caltag) and labeled with an antihuman BCL-2 antibody conjugated to FITC (Becton Dickinson). Cells were analyzed on a FACSCalibur cytometer and analysis was undertaken using the Cell Quest software (Becton Dickinson). At least three independent analysis of each genotype were investigated.

Colony assays. Colony assays were performed using the Methocult medium as recommended by the manufacturer (Stem Cell Technologies) and is described in Supplementary Experimental Procedures.

Apoptosis assays. Apoptosis was assessed by *in situ* detection of fragmented DNA, using the terminal deoxyribonucleotide transferase–mediated nick-end labeling (TUNEL) assay on 5-μm paraffin-embedded liver sections (21). Quantitative data on tissue sections were assessed blindly by two pathologists (A.J. and C.L.) on an Olympus ProvisAX-70 microscope, with wide-field eyepiece number 26.5, providing a field size of 0.344 mm^2 at ×400 magnification. Cell counts were performed on three different fields per section, and expressed as the mean number of cells per field at ×400 magnification using the Olympus SIS software system.

Transplantation of bone marrow and spleen cells. Bone marrow was isolated from both tibias and femurs and spleen cells were harvested from 6- to 10-week-old *MRP8[BCL-2/NRASD12]* mice as described above, pooled and divided (10^7 nucleated cell aliquots per recipient) for i.v. injections into 12 irradiated FVB/N mice. Six- to 8-week-old FVB/N mice were prepared for transplantation by cesium irradiation totaling 10 Gy, divided into two doses 3 to 4 h apart. Successful transfer of the transgene-positive cells was confirmed by PCR. Spleen cells (10^5, 10^6, or 10^7) from *MMTVtTA/TBCL-2/NRASD12* mice were injected i.v. in tail veins of immunocompromised RAG1-deficient mice, which are B-cell and T-cell deficient (22). Mice were followed for survival and some cells were harvested, and blast counts were determined and transferred into secondary or tertiary recipients. Disease was confirmed by blast cell counts, and expression of the $H2^q$ phenotype of FVB/N mice, whereas recipient RAG1-Bl6 mice have $H2^b$ haplotypes, with genotyping of peripheral blood DNA or confirmation of hBCL-2 expression in Lin^- cells by immunofluorescence.

Immunofluorescence and confocal microscopy. Mononuclear cells of murine or human bone marrow were examined as described in Supplementary Experimental Procedures.

RAS activation assays and Western blotting. Procedures were as described in Supplementary Experimental Procedures.

Statistical analysis. Described in Supplementary Experimental Procedures.

Results

Transgenic mice coexpressing BCL-2 and NRASD12 give rise to MDS/AML–like diseases in a promoter context–dependent manner. We sought to test the hypothesis that the development of AML is a multistep process by creating two different models coexpressing *BCL-2* (23) with mutant *NRASD12* (24): (*a*) a tetracycline-regulatable model where BCL-2 expression is conditionally induced by the MMTVtTA transactivator in which the addition of the tetracycline analogue doxycycline down-regulates transgene expression and (*b*) a constitutive animal model where the two transgenes are driven by the myeloid MRP8 promoter.

To create the tetracycline-regulatable model, *TBCL-2* mice were constructed and crossed with the transactivator *MMTVtTA* mice to express BCL-2. *MMTVtTA/TBCL-2* mice have a benign bone marrow although on close examination, an excess of

Figure 1. Triple transgenic *MMTVtTA/TBCL-2/NRASD12* mice develop high-risk MDS, whereas *MRP8[BCL-2/NRASD12]* transgenic mice show AML progression. *A,* H&E-stained bone marrow smears and organ sections showing increased marrow blasts [low-power (*LP*) magnification, ×40] with liver and spleen infiltration in the triple transgenic mice. At high power (*HP*, ×120), representative normal neutrophils are arrowed (*N in black*), as well as dysplastic cells (*D arrowed in black*) and quantified blast cells (*B arrowed in white*). *MRP8[BCL-2/NRASD12]* spleen sections show a reduction and dispersion of the white pulp and increase of the red pulp due to an increase in extramedullary hematopoiesis, also seen in the liver. As previously reported, single *MRP8BCL-2* or *MRP8NRASD12* transgenic mice show no leukemic phenotype in liver and spleen sections during the time of observation of up to 6 mo (24, 49). Nevertheless, the spleens of *MRP8NRASD12* mice are enlarged; this is due to reactive proliferation of cells as a result of their susceptibility to develop infections and not to malignancy. This phenomenon has been previously described as a susceptibility of these mice to develop hyperkeratotic lesions, which become secondarily infected with fecal flora, resulting in the proliferation of myeloid cells (24). Significantly increased blast cell populations were observed in bone marrow samples of single *MRP8BCL-2* versus FVB/N mice ($P < 0.005$; $n = 5$) and *MRP8[BCL-2/NRASD12]* versus FVB/N mice ($P < 0.00005$; $n = 4$). *B,* histograms of blood counts demonstrating increased WBC, reduced platelet counts with unchanged RBC, and increased organ/body weight ratios. *C,* bone marrow immunophenotyping: The *MMTVtTA* promoter drives disease with expansion toward the myeloid compartments (Mac-1/Gr-1), showing in *MMTVtTA/TBCL-2/NRASD12* increased R1 to R2 ratio (*bottom*), thus depicting a blast cell expansion. Representative of three independent experiments. *D,* TUNEL staining of paraffin-embedded liver sections; low-power (×200) and high-power (×600) magnifications show significantly increased apoptosis in *MMTVtTA/TBCL-2/NRASD12* versus controls. Three fields were counted in each of the two mice in each group.

granulated, nondystrophic/pathologic myeloblasts with the capacity to mature was noted (12 ± 2%; $n = 3$; Supplementary Fig. S1*A*), and a survival similar to the wild-type FVB/N mice (data not shown). An *MMTVtTA/TBCL-2* line was crossed with the *MRP8NRASD12MMTVtTA* mice (24) to generate transgenic *MMTVtTA/TBCL-2/NRASD12* mice. The *MRP8NRASD12* mice had dysplastic differentiated bone marrows with normal blood counts (Fig. 1*A*; Supplementary Fig. S1*C*). *MMTVtTA/TBCL-2/NRASD12* mice have increased WBC counts ($P < 0.05$), reduced platelet counts ($P < 0.001$), and enlarged spleens and livers ($P < 0.001$ and $P < 0.05$ compared with FVB/N and MMTVtTA controls; Fig. 1*B*). Morphologically, neutrophils of *MMTVtTA/TBCL-2/NRASD12* mice are dysplastic, with segmented nuclei; some may be vacuolated, with less nuclear appendages and a finer chromatin (Fig. 1*A*). The excess of blasts in the *MMTVtTA/TBCL-2/NRASD12* bone marrow averages 15 ± 3% ($n = 3$; Fig. 1*A*). Compared with wild-type FVB/N, bone marrow immunophenotyping showed an increase in Sca-1^+ cells (data not shown), consistent with the increased marrow blasts, and an increase in Mac-1^+/Gr-1^+ population with higher Mac-1^+/Gr-1^{low} (R1) subpopulations (Fig. 1*C, top* and *bottom*) consistent with the myeloid left shift. The liver sections did not show aggressive invasiveness although there were some infiltrations of myeloblasts. Spleen sections showed reduction and dispersion of the white pulp and increase of the red pulp due to an increase in extramedullary hematopoiesis (Fig. 1*A*). These results indicate that the disease of *MMTVtTA/TBCL-2/NRASD12* mice resembles that of human high-risk MDS [FAB (25) or WHO (26) classifications]; the thrombocytopenia and neutrophil dysplasia do not meet the Bethesda classification criteria for myeloid leukemia but are consistent with MDS (20).

For the generation of the constitutive BCL-2 mice, *MRP8BCL-2* (23) mice were crossed with *MRP8NRASD12* (24) mice. Compared with the *MMTVtTA/TBCL-2/NRASD12* model, a significantly higher percentage of bone marrow blasts is noted (89 ± 4%, $n = 4$) with aggressive invasiveness in the livers and spleens (Fig. 1*A*). Whereas, as previously described (23, 24), *MRP8NRASD12* ($n = 43$) and *MRP8BCL-2* ($n = 65$) transgenic mice have survival patterns resembling wild-type FVB/N mice ($n = 76$); *MRP8[BCL-2/NRASD12]* mice ($n = 31$) have a significantly poorer survival with 50% (16 of 31) dying within 3 to 4 months ($P < 0.0001$; Supplementary Fig. S1*B*). Mortality of these mice is due to a myeloid neoplasm that progressed from MDS to myeloid leukemia without maturation. Before death, blood counts show quantitative abnormalities, among which progressive decrease of platelets is the most indicative (mean 2-fold; $P < 0.001$; Supplementary Fig. S1*C*). With peripheral cytopenia and increased marrow blasts, the disease of the *MRP8[BCL-2/NRASD12]* mice may be classified as human AML-like (FAB and WHO classifications; refs. 25, 26) or murine myeloid leukemia without maturation (Bethesda classification; ref. 20). Immunophenotyping of hematopoietic tissues substantiate the leukemic pathology of the *MRP8[BCL-2/NRASD12]* mice. Compared with wild-type mice, the bone marrow Sca-1^+ population is increased 3.5-fold in the *MRP8[BCL-2/NRASD12]* mice, and 1.5-fold and 2.5-fold in the *MRP8NRASD12* and *MRP8BCL-2* mice, respectively (data not shown). This is also consistent with the observed increase in blast cells in the bone marrow of the single and double MRP8 transgenic mice, with the *MRP8BCL-2* bone marrows revealing a proportion of myeloid blast cells (18 ± 5%, $n = 5$; Fig. 1*A*). Significantly increased bone marrow populations were positive for the myeloid markers, Mac-1 and Gr-1, in the *MRP8NRASD12* and *MRP8[BCL-2/NRASD12]* mice compared with FVB/N wild-type mice, with a highly significant increase in the number of Mac-1^+/Gr-1^{low} myeloid cells (R1) in the double transgenic mice, indicating a left shift in maturation of the Mac-1^+/Gr-1^{low} subpopulation (Supplementary Fig. S1*D, top* and *bottom*), which correlated well with increased bone marrow blast infiltration (Fig. 1*A*).

As MDS is characterized by increased apoptosis of hematopoietic cells, tissues from mouse liver sections were analyzed by a TUNEL assay to further substantiate the observed MDS morphologic features. As expected, increased apoptosis was detected when MDS features were dominant, such as in single *MRP8NRASD12* and *MMTVtTA/TBCL-2/NRASD12* mice; however, no apoptotic cells were noted when blast infiltration was abundant as in the leukemic *MRP8[BCL-2/NRASD12]* mice (Fig. 1*D*). Morphologically, the positive staining cells were hematopoietic.

Consistent with the expanded Sca-1^+ population in both models (data not shown), the leukemic stem cell compartmentalization of these primitive cells were next confirmed by confocal microscopy for exogenous hBCL-2 alongside the Sca-1 and c-Kit markers in Lin$^-$/Sca-1^+/c-Kit$^+$ enriched *MMTVtTA/TBCL-2/NRASD12* bone marrow cells (see Fig. 2*A* for a representative cell). Additionally, Lin$^-$ sorted samples from both MDS-like and AML-like mice showed a significantly raised Sca-1^+/c-Kit$^+$ population versus control mice (Fig. 2*B, top* and *bottom*). A significant increase in myeloid colony numbers was observed in *MMTVtTA/TBCL-2/NRASD12* and *MRP8[BCL-2/NRASD12]* compared with MMTVtTA and FVB/N controls ($P < 0.05$ and $P < 0.005$, respectively; Fig. 2*C*).

The myeloid neoplastic disease of the *MMTVtTA/TBCL-2/NRASD12* was serially transplantable into RAG1 mice as evidenced by blast counts from bone marrow smears (Supplementary Fig. S2*A*). Similarly, the *MRP8[BCL-2/NRASD12]* model was transplantable into RAG1 and lethally irradiated mice as evidenced by pathology (Supplementary Fig. S2*B*) and immunophenotyping (Supplementary Fig. S2*C*). As both *MMTVtTA/TBCL-2/NRASD12* and *MRP8[BCL-2/NRASD12]* mice were serially transplantable in immunocompromised RAG1 mice up to four passages (data not shown), this suggests that in both models the disease originated in a leukemic stem cell. This is reinforced by the observation that unlike the Lin$^+$ populations, Lin$^-$ cells from diseased MDS-like and AML-like mice were transplantable into RAG1 or lethally irradiated FVB/N mice (Supplementary Fig. S2*A* and data not shown). No significant difference between the mice was observed in the other cell populations; the percentage of lymphoid cells in the leukemic *MRP8[BCL-2/NRASD12]* mice was similar to single *MRP8BCL-2* mice (data not shown).

Thus, the coexpression of NRASD12 with BCL-2 in the myeloid cells of these mice results in two models of leukemogenesis: one model of high-risk MDS (*MMTVtTA/TBCL-2/NRASD12*) and one model of AML (*MRP8[BCL-2/NRASD12]*).

BCL-2 is a rate-limiting step. As the two models described suggest that at least two steps (expression of *BCL-2* and mutated *NRAS*) are required for leukemogenesis, we investigated whether extinction of one of these steps reversed the neoplastic disease. To test this, we took advantage of the inducible *MMTVtTA/TBCL-2/NRASD12* model (tetracycline-off, in which the addition of doxycycline down-regulates transgene expression). When doxycycline is withdrawn, *MMTVtTA/TBCL-2/NRASD12* mice die within 2 months (five of five), compared with no death in six mice with doxycycline treatment, and with death of the majority of mice untreated with doxycycline within 6 months ($n = 18$; Fig. 3*A, right*). When we administered doxycycline at week 3 and continued treatment

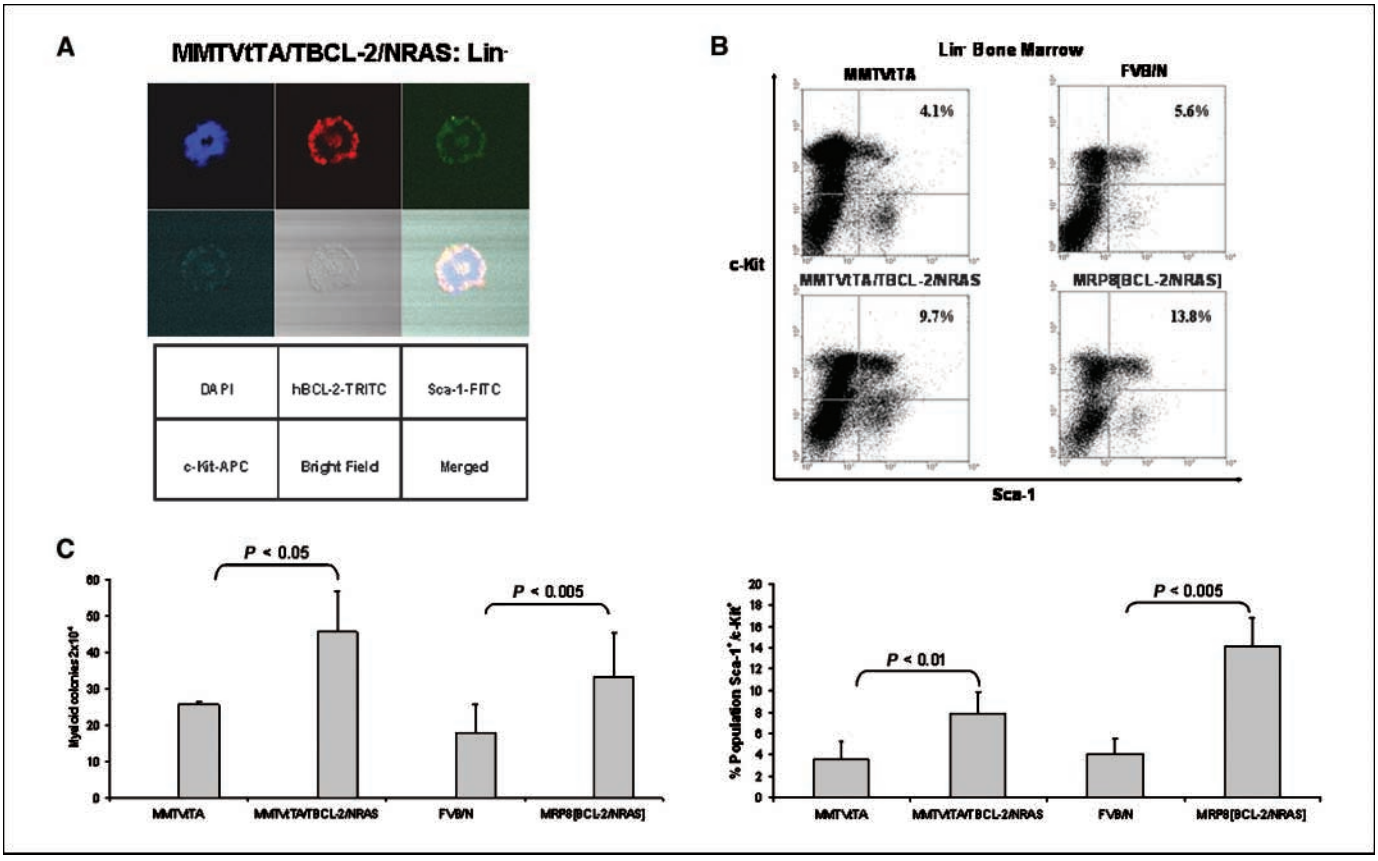

Figure 2. Stem cell compartmentalization of MDS- and AML-like disease models. *A,* confocal microscopy showing colocalization of the transgene hBCL-2 with Sca-1 and c-Kit in representative samples (of three independent experiments) of Lin^-/Sca-1^+/c-Kit^+ sorted bone marrow cells of *MMTVtTA/TBCL-2/NRASD12* (counterstained with 4′,6-diamidino-2-phenylindole). *B, top,* representative immunophenotype trace of Lin^- sorted bone marrow samples from controls and diseased animals (*bottom*) with significant difference in the Sca-1^+/c-Kit^+ population. *Columns,* mean of $n = 5$ *MMTVtTA/TBCL-2/NRASD12* and $n = 3$ *MRP8[BCL-2/NRASD12]* mice analyzed; *bars,* SD. *C,* histogram showing numbers of day 12 to 14 CFU-GM from bone marrows of diseased and normal mice. *Columns,* mean of $n = 7$ *MMTVtTA/TBCL-2/NRASD12* and $n = 5$ *MRP8[BCL-2/NRASD12]* mice analyzed; *bars,* SD.

until week 12, a correction of the disease symptoms, such as thrombocytopenia ($P < 0.001$; Fig. 3*B*) and hyperleukocytosis ($P < 0.005$; Fig. 3*C*), and recovery of normal survival were achieved (Fig. 3*A, right*). Expression of hBCL-2 and the development of the myeloid neoplastic disease could be switched off and on repeatedly by withdrawing or administering doxycycline, respectively, for a maximum of three times over the follow-up period of 22 months with WBC reverting to that of *MRP8NRASD12* mice (Fig. 3*C*). However, although the bone marrow of doxycycline-treated *MMTVtTA/TBCL-2/NRASD12* mice shows a correction of disease with increased survival and a slight but reproducible reduction of bone marrow blast cells (15 ± 3% dropping to 8 ± 3%; $n = 3$; Fig. 3*A, left*), immunophenotyping suggested persistence of bone marrow blast cells with Mac-1^+/Gr-1^{low} cell remaining as high as the untreated mice (data not shown), whereas the Sca-1^+ (as well as the c-Kit^+) population remained unchanged (Fig. 3*D*; Supplementary Fig. S3*A*), indicative of some remaining disease and possibly other steps. Likewise, organs remained infiltrated with immature myeloid cells and spleens were still enlarged (Supplementary Fig. S3*B*) similar in size to *MMTVtTA/TBCL-2/NRASD12* spleens yet distinct from the enlarged reactive spleens of *MRP8NRASD12* mice, which are not infiltrated by blasts (Fig. 1*A, top*; previously described in ref. 24). These persistent abnormalities, despite reduced hBCL-2 expression, suggest that the coexpression of NRASD12 and BCL-2 has driven additional lesions that are irreversible. Nevertheless, the corrections of most of the hematopoietic variables in the absence of hBCL-2 correlated well with a normal life expectancy during a follow-up period of up to 600 days (Fig. 3*A, right*).

BCL-2:RAS-GTP protein complexes occur in the Sca-1^+ compartment of diseased mice. Activating point mutations of *RAS* lock RAS in their GTP-bound active state. As the combination of the *BCL-2* and *NRASD12* transgenes is able to initiate the development of the malignancy in these mice, we asked whether RAS activity was sustained in *MRP8[BCL-2/NRASD12]* and *MMTVtTA/TBCL-2/NRASD12* Sca-1^+ cells coexpressing NRASD12 and BCL-2 and asked whether a common molecular mechanism exists. Within the Sca-1^+ and Mac-1^+ compartments of the spleen cells of *MRP8[BCL-2/NRASD12]* and *MMTVtTA/TBCL-2/NRASD12* mice, increased levels of GTP-bound RAS are present, a finding also noted in the Mac-1^+ sorted populations of the single *BCL-2* and *NRASD12* mice. Expression of hBCL-2 was confirmed using a species-specific antihuman BCL-2 antibody (Fig. 4*A*). Interestingly, in this population, only the phosphorylated form of BCL-2 protein (27) was predominantly observed. RAS activity was assessed using an activation-sensitive pull-down assay, whereby RAS in its GTP-bound configuration is detected via the RAS-binding domain of its downstream effector RAF1 (28, 29). Increased RAS activity was observed in the Sca-1^+ and Mac-1^+ cells of *MMTVtTA/TBCL-2/*

NRASD12 mice, which persisted in the absence of hBCL-2 expression after doxycycline treatment (Fig. 4*A, top*). This may account for the persistence of disease detected by tissue invasion and sustained increase of Sca-1$^+$ cells (Fig. 3*A, left*, and data not shown). Within the Sca-1$^+$ compartment of the *MRP8[BCL-2/NRASD12]* spleen cells, increased levels of GTP-bound RAS are also noted (Fig. 4*A, middle*). Interestingly, hBCL-2 probing of the active RAS pull-down assay proteins revealed the presence of BCL-2 in the RAS complex (BCL-2:RAS-GTP) in untreated *MMTVtTA/TBCL-2/NRASD12* mice (Fig. 4*A, top*). These experiments were also performed with *MMTVtTA/TBCL-2/NRASD12* mice treated with doxycycline for 3 and 12 weeks in which BCL-2 expression is significantly extinguished. The complexes were correlated by a time-dependent decrease of BCL-2. The presence of the BCL-2:RAS-GTP complex was also observed in *MRP8[BCL-2/NRASD12]* mice (Fig. 4*A, middle*). As described above,

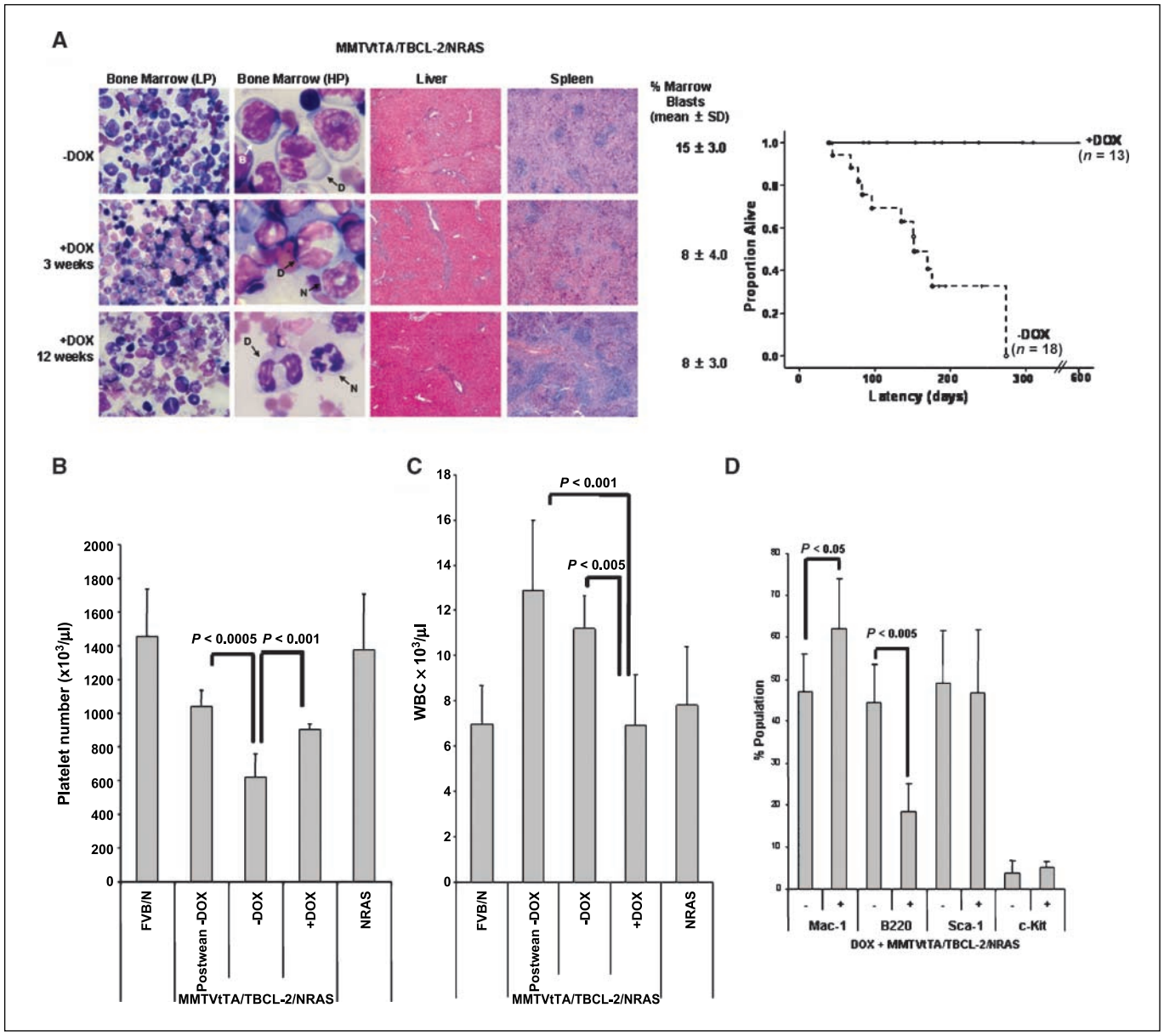

Figure 3. *MMTVtTA/TBCL-2/NRASD12* MDS-like disease is stable after inhibition of BCL-2 expression and rescue from lethality. *A, left,* bone marrow smears and organ sections (H&E stained as in Fig. 1*A*) of mice without (*−DOX*) and with (*+DOX*) doxycycline after 3 and 12 wk illustrate a persistence of marrow blast (visualized at low-power magnification, ×40) and infiltrated liver and spleens. Doxycycline-treated mice have increased mature neutrophils. High-power magnification (×120) of bone marrow show representative normal neutrophils (*N arrowed in black*), dysplastic cells (*arrowed D in black*), and quantified blast cells (*B arrowed in white*). *Right,* Kaplan-Meier survival curves of triple transgenic mice in the absence and presence of doxycycline showing rescue of lethality by switching BCL-2 expression off. *Vertical lines,* censored animals taken off doxycycline. Blood index measurements: after weaning at 3 wk old, 3 to 6 mo from birth, and 3 wk after doxycycline administration. *B,* reduced peripheral blood platelet counts are indicative of disease where rescue was observed with partial recovery of platelet counts in the presence of doxycycline compared with that in the absence of doxycycline. *Columns,* mean (n = 7); *bars,* SD. *C,* with WBC counts after weaning at 3 wk old, in the absence compared with that in the presence of doxycycline. *Columns,* mean (n = 7); *bars,* SD. *D,* histogram of peripheral blood immunophenotyping of the same mice before and after doxycycline treatment of *MMTVtTA/TBCL-2/NRASD12* mice showing expansion of the myeloid and reduced B-cell compartments. The increase in Mac-1 after BCL-2 expression is switched off possibly due to increased myelopoiesis as there is a reduction in B220$^+$ cells, where BCL-2 expression is normally driven by the MMTVtTA. The total Sca-1$^+$ population remains unchanged.

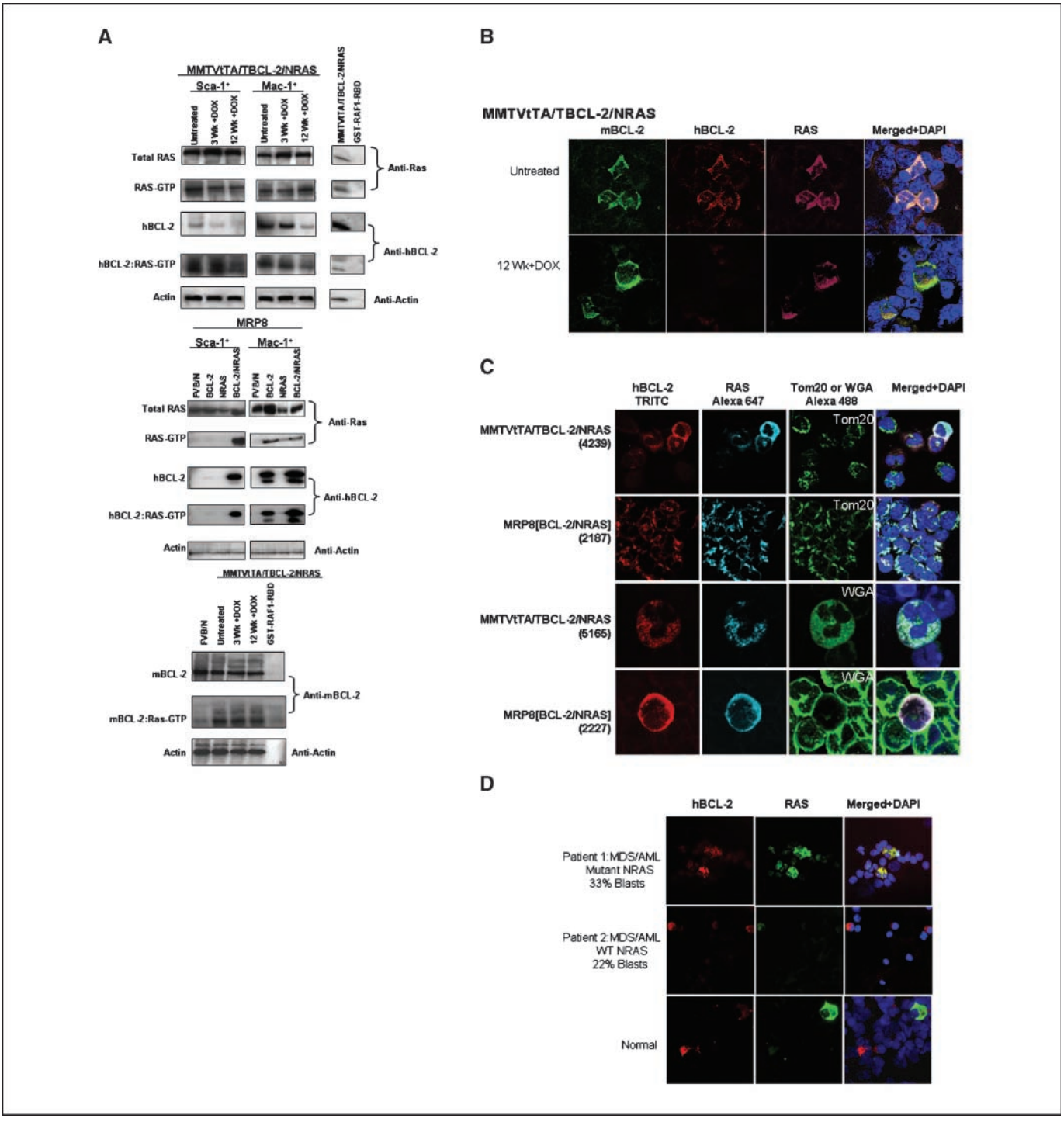

Figure 4. Increased RAS activity in Sca-1$^+$ cells of MRP8[BCL-2/NRASD12] and *MMTVtTA/TBCL-2/NRASD12* mice due to BCL-2:RAS-GTP complexing and colocalization of the complex. *A, top,* Sca-1$^+$ and Mac-1$^+$ sorted spleen cells from *MMTVtTA/TBCL-2/NRASD12* mice without (*Untreated*) or with doxycycline treatment for 3 and 12 wk; *middle,* wild-type FVB/N, *MRP8BCL-2, MRP8NRASD12*, and *MRP8[BCL-2/NRASD12]* mice were assessed for total RAS expression by Western blotting and total BCL-2 expression by reprobing the blots with a human specific anti–BCL-2 antibody (*hBCL-2*). Active RAS-GTP levels were assessed via a sensitive RAF1-RBD pull-down assay followed by Western blotting with an anti-RAS antibody. Blots were reprobed with anti-actin antibody to assess protein loading. Results shown are representative of three independent experiments. *Bottom,* RAF1-RBD pull-down assay of FVB/N, untreated, and doxycycline-treated diseased *MMTVtTA/TBCL-2/NRASD12* mice, demonstrating persistence of mBCL-2:RAS-GTP complex irrespective of hBCL-2 levels. *B,* immunofluorescence microscopy of *MMTVtTA/TBCL-2/NRASD12* mice bone marrow cells shows loss of human BCL-2 (*hBCL-2*) in the presence of doxycycline for 12 wk. *DAPI,* 4′,6-diamidino-2-phenylindole. *C,* confocal microscopy showing subcellular localization of BCL-2:RAS complex. hBCL-2, RAS, and mitochondria (*Tom20*) or plasma membrane (*WGA*) stained cells of unsorted bone marrow cells in *MMTVtTA/TBCL-2/NRASD12* and *MRP8[BCL-2/NRASD12]* mice showing mitochondrial localization of hBCL-2 and RAS in *MRP8[BCL-2/NRASD12]* mice and reduction of mitochondrial colocalization in *MMTVtTA/TBCL-2/NRASD12* mice, with plasma membrane colocalization of *MMTVtTA/TBCL-2/NRASD12* and a reduction of colocalization with WGA in the *MRP8[BCL-2/NRASD12]* mice (representative of at least three independent experiments). *D,* colocalization of BCL-2 and RAS when NRAS is mutated in human samples. Immunofluorescence microscopy of bone marrow cells from patient 1 with a secondary MDS/AML presenting with mutant NRAS, and from patient 2 with secondary MDS/AML with wild-type NRAS and normal human bone marrow. Colocalization of hBCL-2 and RAS is observed only in the presence of mutant NRAS.

after doxycycline treatment, although lethality is rescued, myeloblast infiltration remains. Mechanistically, RAS activity remained high in the Sca-1$^+$ spleen cells even when hBCL-2 is switched off (Fig. 4*A, top*). We therefore hypothesized the recruitment of endogenous mBCL-2 within the complex. RAF1-RBD pull-down assay of FVB/N, untreated, and doxycycline-treated diseased *MMTVtTA/TBCL-2/NRASD12* mice showed persistence of mBCL-2:RAS complex irrespective of hBCL-2 levels (Fig. 4*A, bottom*).

Although *in vitro* interaction between BCL-2 and RAS has been previously reported in Jurkat cells (30) and R-RAS, a RAS-related protein detected with BCL-2 using a yeast two-hybrid system (31), this is the first presentation of data linking the unique presence of BCL-2 in an NRAS-activated complex to the development of a malignant disease. The persistence of activated RAS despite significant decrease of BCL-2 illustrates the initiation of irreversible steps.

Using confocal and immunofluorescence microscopy, we substantiate that hBCL-2 and RAS are colocalized in *MMTVtTA/TBCL-2/NRASD12* and *MRP8[BCL-2/NRASD12]* cells from granulocyte-macrophage colony-forming unit (CFU-GM) colonies as well as unseparated and Lin$^-$ separated bone marrow cell populations (Fig. 4*B* and *C*; Supplementary Fig. S4*A* and *B*). Importantly, we confirm the controlled extinction of the colocalized proteins via immunofluorescence microscopy of *MMTVtTA/TBCL-2/NRASD12* bone marrow cells in the absence of lethality when hBCL-2 expression is turned off with the administration of doxycycline and the persistence of the colocalization of RAS and mouse BCL-2 (Fig. 4*B*).

To identify the subcellular localization of the BCL-2:RAS complex in the *MMTVtTA/TBCL-2/NRASD12* and *MRP8[BCL-2/NRASD12]* mice, triple staining of RAS, BCL-2, and mitochondria or plasma membrane was undertaken (Fig. 4*B* and *C*) and colocalizations were quantified (Supplementary Fig. S4*C*). Despite >50% of the cells of the *MMTVtTA/TBCL-2/NRASD12* with colocalization of RAS and hBCL-2, only a minority of the cells ($\sim$10%) colocalize in the mitochondria, whereas in the *MRP8[BCL-2/NRASD12]* mice, most of the bone marrow cells, which were RAS and hBCL-2 positive, were found to colocalize in the mitochondria (Fig. 4*C* and Supplementary Fig. S4*C*). Bone marrow Lin$^-$ isolated cells confirmed these findings with 50% of BCL-2 and RAS colocalizing, 12% of hBCL-2 colocalizing with mitochondria, and nearly no RAS colocalizing in the mitochondria (1%) of the *MMTVtTA/TBCL-2/NRASD12* mice, whereas 30% of *MRP8[BCL-2/NRASD12]* cells with hBCL-2 and RAS colocalized, 20% of the hBCL-2 colocalized with mitochondria, and practically all of the RAS in the complex appeared to localize in the mitochondria (25%; Supplementary Fig. S4*B* and *C*). In contrast, with the plasma membrane probe wheat germ agglutinin (WGA), we observed hBCL-2 and RAS colocalizations in the *MMTVtTA/TBCL-2/NRASD12* mice of around 40% and a reduction in the *MRP8[BCL-2/NRASD12]* mice at $\sim$7% (Supplementary Fig. S4*C*).

To confirm the relevance of this observation in human MDS/AML, we analyzed the coexpression of BCL-2 and RAS in the mononuclear cells of the bone marrow of MDS/AML patients (n = 6) with known *RAS* mutation status (32). Interestingly, colocalizations of BCL-2 and RAS in MDS/AML patient samples but not in a normal individual was also observed (Fig. 4*D*). The colocalization of BCL-2 and RAS appears to be correlated with the mutated status of RAS (n = 2 with RAS mutations and n = 3 wild-type). Although these preliminary results require confirmation on a larger cohort of MDS/AML patients, such an association in the pathogenesis of MDS/AML patients has not been previously described.

To further dissect the mechanisms involved, we interrogated the mitogen-activated protein kinase and AKT signaling pathways in Mac-1 and Sca-1 sorted bone marrow cells from diseased animals versus healthy controls (Fig. 5). We used previously reported optimized conditions by others and ourselves (33, 34). In the *MMTVtTA/TBCL-2/NRASD12* cells, the proapoptotic phenotype corresponds with the reduced levels of phosphorylated-AKT, with increased phosphorylated extracellular signal-regulated kinase (ERK) compared with the MMTVtTA in the Sca-1$^+$ compartment (Fig. 5*A*). Furthermore, phosphorylated ERK is up-regulated in the *MRP8NRASD12* single transgenic line as well as the Mac-1$^+$ compartment of the *MRP8[BCL-2/NRASD12]* (Fig. 5*B*). In the Sca-1$^+$ compartment, where we postulate that BCL-2 is dominant based on its apoptosis profile, phosphorylated AKT is up-regulated, consistent with the antiapoptotic characteristics of cells from this line (Fig. 5*B*).

Discussion

We have created two murine models of initiation and progression of human MDS/AML, using two candidate genes, mutant *NRAS* and *BCL-2*. Both have previously been identified by us and others as risk factors for AML in MDS patients (9, 10, 16, 17). The *MMTVtTA/TBCL-2/NRASD12* mouse model represents human MDS, whereas the constitutive *MRP8[BCL-2/NRASD12]* model is closer to AML. This distinction is also reflected by the presence of apoptosis (as observed in the human low-risk MDS stage of the disease) seen in the hematopoietic tissues in the livers of *MMTVtTA/TBCL-2/NRASD12* mice and its decreased presence or absence in the *MRP8[BCL-2/NRASD12]* mice (as in the human high risk MDS and AML), which is also reflected by the signaling profiles of these mice. Furthermore, the subcellular localization of the two oncogenes when complexed appears to be consistent with their apoptotic characteristics. In the MDS-like mice, which like single

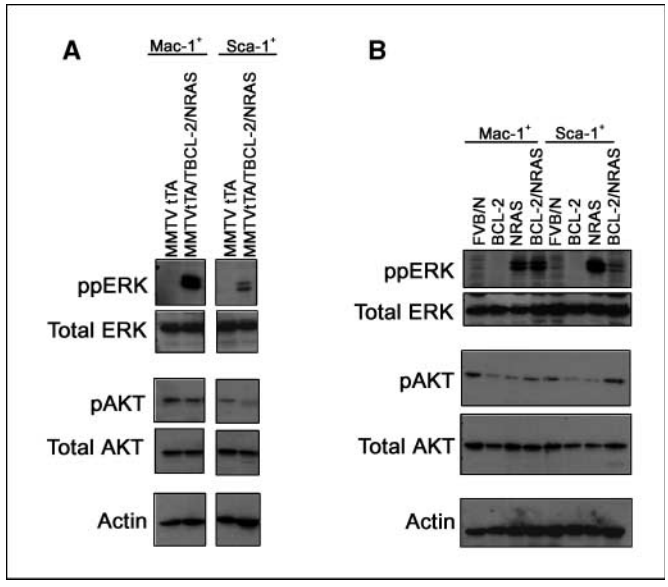

Figure 5. Regulation of ERK and AKT signaling in MDS/AML–like mice. Mac-1$^+$ and Sca-1$^+$ spleen cells from control and diseased MDS (*A*) and AML (*B*) animals were incubated for 4 h in the presence of WEHI-conditioned/serum-rich medium, harvested, and lysed for protein extraction. Western blot analysis was carried out for phosphorylation-specific and total ERK and AKT levels, and normalized protein loading was confirmed by probing for actin.

transgenic *MRP8NRASD12* mice are proapoptotic, the majority of the RAS and BCL-2 doubly stained cells did not colocalize in the mitochondria, but localized to the plasma membrane, where active RAS is normally located, whereas in the AML-like disease RAS and BCL-2 colocalize more so in the mitochondria, where BCL-2 is normally found and is consistent with the antiapoptotic properties of BCL-2. Interestingly, in Madin-Darby canine kidney cells and Jurkat T-cells, protein kinase C (PKC) agonists have been found to induce mutant KRAS to dissociate from the plasma membrane where activated RAS proteins are normally found and to translocate to the mitochondria where it associates with BCL-XL to stimulate apoptosis (35). Although mutant KRAS was found to associate with BCL-2, this interaction was found to be insensitive to PKC agonists. The difference in our findings in the AML-like mice, which appear to complex NRASD12 and BCL-2 in the mitochondria to give rise to reduced apoptosis, may be due to the different cell types and context. The coexpression of these two genes is necessary for the disease to appear as both of the single transgenic mice, *NRASD12* or *BCL-2*, have mild phenotypes and normal survival. The stem cell features of these diseases are defined by their ability to repopulate immunodeficient RAG1 or lethally irradiated mice. This is confirmed by the finding that the disease of the *MMTVtTA/TBCL-2/NRASD12* and *MRP8[BCL-2/NRASD12]* mice can be successfully transplanted into RAG1 or lethally irradiated FVB/N mice using Lin^- isolated cells in the absence of disease or repopulation from the Lin^+ fraction. Furthermore, there are increased primitive Sca-1^+, Mac-1^+/Gr-1^{low}, and Lin^-/Sca-1^+/c-Kit^+ bone marrow cell populations in both mice, and an increase in progenitors compared with wild-type mice, indicating diseases of primitive cells. Indeed, hBCL-2 expression was observed in bone marrow of Lin^-/Sca-1^+/c-Kit^+ sorted cells from *MMTVtTA/TBCL-2/NRASD12* mice, showing that the mouse mammary tumor virus–long terminal repeat (MMTV-LTR) can drive expression to this primitive compartment. Furthermore, the *MRP8[BCL-2/NRASD12]* and the *MMTVtTA/TBCL-2/NRASD12* mice also present with enlarged infiltrated spleens and liver characteristic of malignant cells. Sca-1 directed BCL-2 overexpression in the aorta-gonad-mesonephros region, wherein the mouse embryo first hematopoietic stem cells are generated, and also results in increased numbers of Sca-1^+ and c-Kit^+ cells (36). We have shown that expression of BCL-2 in human myeloid progenitors blocks differentiation (18). In the single transgenic *BCL-2* mouse, we have noted some immature Sca-1^+ cells and marrow blasts. *NRASD12* mice show myeloid dysplastic features but no expansion of the Sca-1^+ population and no blast infiltration with well-differentiated cells. Few other abnormalities are seen and, thus, both the single *NRASD12* mouse and the single *BCL-2* mouse have a normal phenotype and survival. We surmise that in the MRP8-targeted myeloid progenitor, the combined effects of constitutively active *NRASD12* and expression of active BCL-2 lead to an expansion of immature myeloid cells at the expense of differentiation. Therefore, it would appear that MMTV-LTR and MRP8, which do not usually target hematopoietic stem cells, in the context of the BCL-2:RAS-GTP complex give rise to leukemic stem cells. However, the target cells may be different depending on where BCL-2 is expressed; either the mutant NRAS is dominant and the cells fail to differentiate and die by apoptosis, giving rise to a human MDS-like disease (*MMTVtTA/TBCL-2/NRASD12*), or antiapoptotic BCL-2 is dominant, leading to a block in differentiation and a reduction in apoptosis, and blast cells accumulate, giving a human AML-like disease (*MRP8[BCL-2/NRASD12]*).

The activation-sensitive GST-RAF1-RBD immunoprecipitation assays allowing quantification of active RAS levels showed that, indeed, activated RAS in the Sca-1^+ compartment is only detected in the *MRP8[BCL-2/NRASD12]* and the *MMTVtTA/TBCL-2/NRASD12* transgenic mice and not in the single *NRASD12, BCL-2*, or normal FVB-N mice, which suggests that the activity of this complex in a primitive compartment may be contributing to disease progression. The elevated total RAS and RAS-GTP levels in the diseased transgenic mice might be due to BCL-2–mediated increased survival of cells that express high levels of NRASD12, which might otherwise undergo cell cycle arrest or senescence. Interestingly, only the phosphorylated form of BCL-2 is found in this cell population where RAS is activated. Investigation of the molecular mechanisms involved within the increased primitive Sca-1^+ cell population revealed the first *ex vivo* identification of the BCL-2:RAS-GTP complex in the context of the disease, suggesting that the association between these oncoproteins may mediate an underlying mechanism. Extinction of one of these genes, *BCL-2*, rescues the lethality of the disease. A preliminary study of patient samples lead to the discovery of a similar colocalization in the bone marrow of patients with MDS/AML harboring a mutated NRAS. Although the role of phosphorylated BCL-2 is controversial (37), these observations provide further insight into the mechanisms by which association of activated RAS with BCL-2 is context dependent in the transduction of proapoptotic versus antiapoptotic signaling during hematopoietic development. This is consistent with the signaling profile where ERK is increased with decreased AKT in the RAS-mediated proapoptotic MDS-like mice and AKT is increased in the BCL-2–mediated antiapoptotic AML-like disease.

Numerous *in vivo* murine RAS models have been reported presenting with different diseases. Models established with either viral *Ha-ras* or with *Ha-ras* driven by a Moloney murine leukemia virus LTR as well as transgenic mice established with a codon 61 mutant *NRAS* (38–41) present with proliferative lymphoid diseases. Furthermore, transplantation of bone marrow cells retrovirally transduced with *NRASD12* (42) or mutant *KRAS* conditionally expressed in Mx1^+ cells result in myeloproliferative disorders (34, 43). The last two models are particularly elegant in that despite the physiologic levels of mutant KRAS driven by its own promoter, alone a lethal disease ensues rapidly due to the Mx1 targeting a different progenitor to the MRP8-driven NRASD12 used in our present study. Tetracycline-regulatable mutant *NRASV12* mice crossed with VAVtTA mice results in a reversible systemic mastocytosis in 2 to 4 months (44). Thus, distinct phenotypes may be obtained, implying that the *in vitro* structure/context–dependent effect of the different RAS proteins is also reflected *in vivo*. *NRASD12* is one of the most frequent mutations found in MDS or AML. Both MDS and AML affect the myeloid stem cells and therefore justifies the use of a myeloid promoter, such as MRP8. As the MRP8 promoter is a target of C/EBPα in human CD34$^+$ cells, the concomitant-driven expression of both transgenes in the primitive Sca-1^+ compartment is to be expected (45). The models established in this study closely mimic the human MDS/AML. MRP8 appears to be turned on in a subset of granulocyte/macrophage progenitors (46), and it would appear that granulocyte/macrophage progenitors can become leukemic stem cells (47–49).

Whereas these two models provide insights into the leukemogenesis of the patients through the required cooperation of these two disease candidate genes to expand the primitive compartment to form leukemic stem cells, the regulatable *MMTVtTA/TBCL-2/NRASD12* model shows that the expression of BCL-2 is necessary

for both initiation and progression of malignancy; BCL-2 accelerates the development of neoplasia in these models as it does in other mouse models of acute promyelocytic and chronic myelogenous leukemia (47, 48). However, close analysis of the hematopoietic compartments shows the irreversibility of some variables such as the persistence of elevated Sca-1$^+$ population in the peripheral blood, blasts in the bone marrow, and splenomegaly with infiltration of the liver, and thus indicates that although extinction of BCL-2 expression rescues from lethality, some degree of disease still exists, consistent with the multistep mechanisms involved in a progressive disease like MDS. In our model, we hypothesize that mutant NRAS can recruit mBCL-2 to remain active. We provide evidence from the pull-down and confocal assays to show that mouse BCL-2 binds with active RAS and colocalizes with RAS. The complex association of BCL-2 with active RAS may lead to irreversible steps if mBCL-2 and NRAS are left to cooperate until overt leukemia appears.

We have shown that at least two candidate oncogenes (*BCL-2* and mutant *NRAS*) can cooperate to give rise to malignant disease with a penetrance of around 80% and a latency period of 3 to 6 months. The demonstration that one of them (*BCL-2*) is a rate-limiting step may therefore be a target for future therapy in this group of diseases. This study validates an *in vivo* strategy to create molecularly defined multistep models with specific gene abnormalities that cause a disease with hallmarks of MDS and that transform to AML. These models will be important to decipher the BCL-2:RAS-GTP complex and the contribution of other genetic abnormalities that may accelerate disease progression, and to test novel therapeutic approaches.

Acknowledgments

Received 1/16/2007; revised 9/6/2007; accepted 10/15/2007.

Grant support: Fulbright Commission, Welsh Bone Marrow Transplant Fund, UK Leukaemia Research Fund, Kay Kendall Research Fund, Eli Lilly International Foundation, ARECA, Fondation de France, European Leukemia Network, NIH, and Institut National de la Sante et de la Recherche Medicale; and NIH (D. Felsher).

The costs of publication of this article were defrayed in part by the payment of page charges. This article must therefore be hereby marked *advertisement* in accordance with 18 U.S.C. Section 1734 solely to indicate this fact.

Scott Kogan is a Scholar of the Leukemia and Lymphoma Society.

We thank Michael Bishop for hosting the early part of this study; Jack Whittaker for reviewing the hematologic slides; Christopher Marshall (Institute for Cancer Research, London, United Kingdom) for providing the pGEX-2T-RAF1-RAS construct; Fabien Zassadowski, Thi-Hai Phan, Macarena Robledo, Sacha Muszlak, Liesbeth Mudder, Katerina Pokorna, Aurore Cleret, and Lucie Da Silva for technical assistance; members of the Institut Universitaire d'Hématologie IFR105 specifically the Département d'Experimentation Animale, Bernard Boursin from the photography laboratory, Chrystelle Doliger of the Imagery Department for the confocal microscopy, who are supported by grants from the Conseil Regional d'Ile-de-France, and the Ministère de la Recherche.

The authors have no conflicting financial interest.

References

1. Knudson AG, Jr. Mutation and cancer: statistical study of retinoblastoma. Proc Natl Acad Sci U S A 1971;68:820–3.
2. Vogelstein B, Kinzler KW. The multistep nature of cancer. Trends Genet 1993;9:138–41.
3. Pitot HC, Dragan YP. Facts and theories concerning the mechanisms of carcinogenesis. FASEB J 1991;5:2280–6.
4. Gerl R, Vaux DL. Apoptosis in the development and treatment of cancer. Carcinogenesis 2005;26:263–70.
5. Jackson-Grusby L. Modeling cancer in mice. Oncogene 2002;21:5504–14.
6. Pelengaris S, Khan M, Evan G. c-MYC: more than just a matter of life and death. Nat Rev Cancer 2002;2:764–76.
7. Carter G, Hughes DC, Clark RE, et al. RAS mutations in patients following cytotoxic therapy for lymphoma. Oncogene 1990;5:411–6.
8. Taylor C, McGlynn H, Carter G, et al. RAS and FMS mutations following cytotoxic therapy for childhood acute lymphoblastic leukaemia. Leukemia 1995;9:466–70.
9. Gallagher A, Darley R, Padua RA. RAS and the myelodysplastic syndromes. Pathol Biol (Paris) 1997;45:561–8.
10. Padua RA, Guinn BA, al Sabah AI, et al. RAS, FMS and p53 mutations and poor clinical outcome in myelodysplasias: a 10-year follow-up. Leukemia 1998;12:887–92.
11. Padua RA, McGlynn A, McGlynn H. Molecular, cytogenetic and genetic abnormalities in MDS and secondary AML. Cancer Treat Res 2001;108:111–57.
12. Darley RL, Hoy TG, Baines P, Padua RA, Burnett AK. Mutant N-RAS induces erythroid lineage dysplasia in human CD34$^+$ cells. J Exp Med 1997;185:1337–47.
13. McGlynn AP, Padua RA, Burnett AK, Darley RL. Alternative effects of RAS and RAF oncogenes on the proliferation and apoptosis of factor-dependent FDC-P1 cells. Leuk Res 2000;24:47–54.
14. Ho AY, Pagliuca A, Kenyon M, et al. Reduced-intensity allogeneic hematopoietic stem cell transplantation for myelodysplastic syndrome and acute myeloid leukemia with multilineage dysplasia using fludarabine, busulphan, and alemtuzumab (FBC) conditioning. Blood 2004;104:1616–23.
15. Parker JE, Mufti GJ. The myelodysplastic syndromes: a matter of life or death. Acta Haematol 2004;111:78–99.
16. Karakas T, Maurer U, Weidmann E, Miething CC, Hoelzer D, Bergmann L. High expression of bcl-2 mRNA as a determinant of poor prognosis in acute myeloid leukemia. Ann Oncol 1998;9:159–65.
17. Karakas T, Miething CC, Maurer U, et al. The coexpression of the apoptosis-related genes bcl-2 and wt1 in predicting survival in adult acute myeloid leukemia. Leukemia 2002;16:846–54.
18. Plenchette S, Cathelin S, Rebe C, et al. Translocation of the inhibitor of apoptosis protein c-IAP1 from the nucleus to the Golgi in hematopoietic cells undergoing differentiation: a nuclear export signal-mediated event. Blood 2004;104:2035–43.
19. Zinkel SS, Ong CC, Ferguson DO, et al. Proapoptotic BID is required for myeloid homeostasis and tumor suppression. Genes Dev 2003;17:229–39.
20. Kogan SC, Ward JM, Anver MR, et al. Bethesda proposals for classification of nonlymphoid hematopoietic neoplasms in mice. Blood 2002;100:238–45.
21. Gavrieli Y, Sherman Y, Ben Sasson SA. Identification of programmed cell death *in situ* via specific labeling of nuclear DNA fragmentation. J Cell Biol 1992;119:493–501.
22. Mombaerts P, Iacomini J, Johnson RS, Herrup K, Tonegawa S, Papaioannou VE. RAG-1-deficient mice have no mature B and T lymphocytes. Cell 1992;68:869–77.
23. Lagasse E, Weissman IL. bcl-2 inhibits apoptosis of neutrophils but not their engulfment by macrophages. J Exp Med 1994;179:1047–52.
24. Kogan SC, Lagasse E, Atwater S, et al. The PEBP2βMYH11 fusion created by Inv(16)(p13;q22) in myeloid leukemia impairs neutrophil maturation and contributes to granulocytic dysplasia. Proc Natl Acad Sci U S A 1998;95:11863–8.
25. Bennett JM, Catovsky D, Daniel MT, et al. Proposals for the classification of the myelodysplastic syndromes. Br J Haematol 1982;51:189–99.
26. Vardiman JW, Harris NL, Brunning RD. The World Health Organization (WHO) classification of the myeloid neoplasms. Blood 2002;100:2292–302.
27. Ito T, Deng X, Carr B, May WS. Bcl-2 phosphorylation required for anti-apoptosis function. J Biol Chem 1997;272:11671–3.
28. van Triest M, de Rooij J, Bos JL. Measurement of GTP-bound Ras-like GTPases by activation-specific probes. Methods Enzymol 2001;333:343–8.
29. Ingram DA, Hiatt K, King AJ, et al. Hyperactivation of p21(ras) and the hematopoietic-specific Rho GTPase, Rac2, cooperate to alter the proliferation of neurofibromin-deficient mast cells *in vivo* and *in vitro*. J Exp Med 2001;194:57–69.
30. Chen CY, Faller DV. Phosphorylation of Bcl-2 protein and association with p21Ras in Ras-induced apoptosis. J Biol Chem 1996;271:2376–9.
31. Fernandez-Sarabia MJ, Bischoff JR. Bcl-2 associates with the ras-related protein R-ras p23. Nature 1993;366:274–5.
32. Bowen DT, Frew ME, Hills R, et al. RAS mutation in acute myeloid leukemia is associated with distinct cytogenetic subgroups but does not influence outcome in patients younger than 60 years. Blood 2005;106:2113–9.
33. Omidvar N, Pearn L, Burnett AK, Darley RL. Ral is both necessary and sufficient for the inhibition of myeloid differentiation mediated by Ras. Mol Cell Biol 2006;26:3966–75.
34. Braun BS, Tuveson DA, Kong N, et al. Somatic activation of oncogenic Kras in hematopoietic cells initiates a rapidly fatal myeloproliferative disorder. Proc Natl Acad Sci U S A 2004;101:597–602.
35. Bivona TG, Quatela SE, Bodemann BO, et al. PKC regulates a farnesyl-electrostatic switch on K-Ras that promotes its association with Bcl-XL on mitochondria and induces apoptosis. Mol Cell 2006;21:481–93.
36. Orelio C, Harvey KN, Miles C, Oostendorp RAJ, van der Horn K, Dzierzak E. The role of apoptosis in the development of AGM hematopoietic stem cells revealed by Bcl-2 overexpression. Blood 2004;103:4084–92.
37. Agostinis P. Bcl2 phosphorylation: a tie between cell survival, growth, and ROS. Blood 2003;102:3079.
38. Hawley RG, Fong AZ, Ngan BY, Hawley TS. Hematopoietic transforming potential of activated ras in chimeric mice. Oncogene 1995;11:1113–23.
39. Dunbar CE, Crosier PS, Nienhuis AW. Introduction of an activated RAS oncogene into murine bone marrow lymphoid progenitors via retroviral gene transfer results in thymic lymphomas. Oncogene Res 1991;6:39–51.
40. Mangues R, Symmans WF, Lu S, Schwartz S, Pellicer A. Activated N-ras oncogene and N-ras proto-oncogene act through the same pathway for *in vivo* tumorigenesis. Oncogene 1996;13:1053–63.

41. Sinn E, Muller W, Pattengale P, Tepler I, Wallace R, Leder P. Coexpression of MMTV/v-Ha-ras and MMTV/c-myc genes in transgenic mice: synergistic action of oncogenes *in vivo*. Cell 1987;49:465–75.
42. MacKenzie KL, Dolnikov A, Millington M, Shounan Y, Symonds G. Mutant N-ras induces myeloproliferative disorders and apoptosis in bone marrow repopulated mice. Blood 1999;93:2043–56.
43. Chan IT, Kutok JL, Williams IR, et al. Conditional expression of oncogenic K-ras from its endogenous promoter induces a myeloproliferative disease. J Clin Invest 2004;113:528–38.
44. Wiesner SM, Jones JM, Hasz DE, Largaespada DA. Repressible transgenic model of NRAS oncogene-driven mast cell disease in the mouse. Blood 2005;106:1054–62.
45. Cammenga J, Mulloy JC, Berguido FJ, MacGrogan D, Viale A, Nimer SD. Induction of C/EBPα activity alters gene expression and differentiation of human $CD34^+$ cells. Blood 2003;101:2206–14.
46. Passegue E, Wagner EF, Weissman IL. JunB deficiency leads to a myeloproliferative disorder arising from hematopoietic stem cells. Cell 2004;119:431–43.
47. Jaiswal S, Traver D, Miyamoto T, Akashi K, Lagasse E, Weissman IL. Expression of BCR/ABL and BCL-2 in myeloid progenitors leads to myeloid leukemias. Proc Natl Acad Sci U S A 2003;100:10002–7.
48. Kogan SC, Brown DE, Shultz DB, et al. BCL-2 cooperates with promyelocytic leukemia retinoic acid receptor α chimeric protein (PMLRARα) to block neutrophil differentiation and initiate acute leukemia. J Exp Med 2001;193:531–43.
49. Traver D, Akashi K, Weissman IL, Lagasse E. Mice defective in two apoptosis pathways in the myeloid lineage develop acute myeloblastic leukemia. Immunity 1998;9:47–57.